



**HAL**  
open science

## Degradation processes of brominated flame retardants dispersed in high impact polystyrene under UV–visible radiation

Hanene Oumeddour, Hussam Aldoori, Zohra Boubberka, Venkateswara Rao Mundlapati, Vikas Madhur, Corinne Foissac, Philippe Supiot, Yvain Carpentier, Michael Ziskind, Cristian Focsa, et al.

### ► To cite this version:

Hanene Oumeddour, Hussam Aldoori, Zohra Boubberka, Venkateswara Rao Mundlapati, Vikas Madhur, et al.. Degradation processes of brominated flame retardants dispersed in high impact polystyrene under UV–visible radiation. Waste Management and Research, In press, 10.1177/0734242x231219626 . hal-04491723

**HAL Id: hal-04491723**

**<https://hal.science/hal-04491723>**

Submitted on 8 Mar 2024

**HAL** is a multi-disciplinary open access archive for the deposit and dissemination of scientific research documents, whether they are published or not. The documents may come from teaching and research institutions in France or abroad, or from public or private research centers.

L'archive ouverte pluridisciplinaire **HAL**, est destinée au dépôt et à la diffusion de documents scientifiques de niveau recherche, publiés ou non, émanant des établissements d'enseignement et de recherche français ou étrangers, des laboratoires publics ou privés.



Distributed under a Creative Commons Attribution 4.0 International License

# Degradation processes of brominated flame retardants dispersed in high impact polystyrene under UV–visible radiation


Waste Management & Research  
1–12

© The Author(s) 2023



Article reuse guidelines:  
sagepub.com/journals-permissions  
DOI: 10.1177/0734242X231219626  
journals.sagepub.com/home/wmr



Hanene Oumeddour<sup>1</sup>, Hussam Aldoori<sup>1,2</sup>, Zohra Bouberka<sup>2</sup>, Venkateswara Rao Mundlapati<sup>3</sup> , Vikas Madhur<sup>3</sup>, Corinne Foissac<sup>1</sup>, Philippe Supiot<sup>1</sup> , Yvain Carpentier<sup>3</sup> , Michael Ziskind<sup>3</sup>, Cristian Focsa<sup>3</sup> and Ulrich Maschke<sup>1</sup> 

## Abstract

In order to protect human health and the environment, several regulations have been introduced in recent years to reduce or even eliminate the use of some brominated flame retardants (BFRs) due to their toxicity, persistence and bioaccumulation. Dispersions of these BFRs in polymers are widely used for various applications. In this report, four different brominated molecules, decabromodiphenyl ether (DBDE), hexabromocyclododecane (HBCDD), decabromodiphenyl ethane (DBDPE) and tris(tribromophenoxy)triazine (TTBPT), were dispersed in the solid matrix of an industrial polymer, high impact polystyrene (HIPS). The possibility of degradation of these BFRs within HIPS under UV–visible irradiation in ambient air was investigated. The degradation kinetics of DBDE and HBCDD were followed by Fourier transform infrared spectroscopy (FTIR) and high-resolution two-step laser mass spectrometry (L2MS). The thermal properties of the pristine and irradiated polymer matrix were monitored by thermogravimetric analysis (TGA) and differential scanning calorimetry (DSC), which showed that these properties were globally preserved. Volatile photoproducts from the degradation of DBDE, DBDPE and TTBPT were identified by headspace gas chromatography/mass spectrometry analysis. Under the chosen experimental conditions, BFRs underwent rapid degradation after a few seconds of irradiation, with conversions exceeding 50% for HIPS/DBDE and HIPS/HBCDD systems.

## Keywords

Decabromodiphenyl ether, hexabromocyclododecane, novel brominated flame retardants, high impact polystyrene, photodegradation, e-waste

Received 28th April 2023, accepted 16th October 2023 by Editor in Chief Arne Ragossnig.

## Introduction

Brominated flame retardants (BFRs) have attracted particular attention in recent years both because of their widespread use in the fire protection in textiles, building materials and insulation, automotive equipment and electrical and electronic equipment (EEE) (Alaee, 2003; Baumgartner et al., 2013; Ling et al., 2022), and because of the growing concerns about their effects on human health and the environment (Currier et al., 2020; Klinčić et al., 2020). Polybrominated diphenyl ethers (PBDEs) as BFRs form a family of 209 theoretical congeners with different degrees of bromination (Pietroń and Małagocki, 2017).

These synthetic organic compounds are semi-volatile, non-hydrolysable, resistant to acids and bases and generally poorly reactive. This explains their bioaccumulation in different environmental compartments such as sediments and sewage sludge (Morris et al., 2004), air samples and water bodies (Covaci et al., 2003; Li et al., 2023) and in non-human organisms (Couderc et al., 2015; Sühring et al., 2013). As a result, these toxic molecules bioaccumulate in the food chain and threaten the population

through food consumption, ingestion of indoor dust and inhalation of indoor air (He et al., 2018). Decabromodiphenyl ether (DBDE) was one of the most widely used and produced BFRs in the past. After it was banned because of its toxicity, hexabromocyclododecane (HBCDD) replaced DBDE because of its effectiveness in preventing the spread of fire. HBCDD was the third most used BFR after tetrabromobisphenol-A (TBBP-A) and DBDE (Panda et al., 2020) until it was listed as a persistent organic pollutant (POP) by the Conference of the Parties (COPs)

<sup>1</sup>University Lille, CNRS, INRAE, Centrale Lille, UMR 8207 – UMET – Materials and Transformations Unit, Lille, France

<sup>2</sup>Physical Chemistry of Materials-Catalysis and Environment Laboratory, University of Science and Technology of Oran, Oran, Algeria

<sup>3</sup>University Lille, CNRS, UMR 8523 – Physique des Lasers Atomes et Molécules, Lille, France

## Corresponding author:

Ulrich Maschke, UMET, Université de Lille, Bâtiment C6, Cité Scientifique, Villeneuve d'Ascq Cedex 59655, France.  
Email: ulrich.maschke@univ-lille.fr

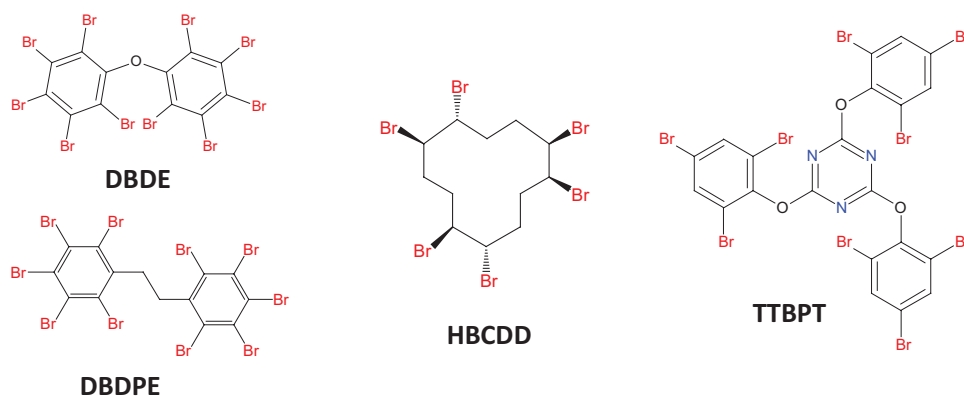


**Figure 1.** Chemical structures of each considered BFRs.

to the Stockholm Convention (SC) on POPs in 2013 (Koch et al., 2015). However, HBCDD can still be used until 2024 under certain circumstances. Thus, other additives have appeared on the market as new BFRs: decabromodiphenyl ethane (DBDPE) and tris(tribromophenoxy)triazine (TTBPT) (Guo et al., 2018; Wu et al., 2012).

Despite restrictions on the use of DBDE, it is still present in large quantities in plastics found in waste EEE (WEEE) (Wäger et al., 2012). According to Taurino et al. (2010), WEEE contains between 10% and 30% of plastics. Hennebert and Filella (2018) estimated that all plastic fractions may contain significant concentrations of BFRs ( $>2000 \text{ mg kg}^{-1}$ ). More recently, Hou et al. (2021) have shown that the new BFRs have similar bioaccumulation properties to PBDEs and are resistant to biotic and abiotic degradation. Waiyarat et al. (2022) reported the presence of HBCDD in dust from cars, homes and offices. In addition, work by Drage et al. (2019) has shown that HBCDD has been found in human serum. More recently, DBDPE and TTBPT have been detected in the environment, indoor air, dust, consumer products and food (Wang et al., 2019; Zuiderveen et al., 2020). On the other hand, the impact of these molecules on human health remains poorly understood. Wang et al. (2022) found that DBDPE causes locomotor neurotoxicity and a potential increased risk of Alzheimer's disease.

The recycling of plastics from WEEE cannot take place without prior treatment to ensure the elimination of toxic molecules. Halogenated aromatic compounds in general have the ability to degrade into lighter molecules when exposed to UltraViolet (UV)–visible light (Gherdaoui et al., 2021; Touaa et al., 2020). A sufficient amount of absorbed electromagnetic energy triggers homolytic cleavage of the C–Br bond and causes structural rearrangements, including cleavage of the ether bond (Saeed et al., 2020). Photolysis is an important transformation pathway for the fate of organobromine molecules. Much research has been done on PBDEs, especially DBDE, revealing its debromination pathway and photolytic products, especially in liquid medium (Eriksson et al., 2004a; Pan et al., 2016). The work of Eriksson and his collaborators (Christiansson et al., 2009; Eriksson et al., 2004b) has shown that PBDEs degrade in organic and aquatic media, forming mainly mixtures of lower brominated PBDEs, but also hydroxylated polybrominated dibenzofurans (PBDF-OH) and

bromophenols. In contrast, little work has been done on the photolysis of DBDEs in solid media. Kajiwara et al. (2008, 2013) confirmed the photodegradation of DBDE in a high impact poly(styrene) (HIPS) polymer matrix under sunlight exposure for 150 days in partial debromination to nona- and octa-BDE, but polybrominated diphenyl ether (PBDE) congeners such as BDE-47, 99 and 100 were not formed. Khaled et al. (2018a, 2018b) reported that the presence of bromine in the polymer accelerated the photooxidation of the polymer under sunlight exposure, preventing the complete degradation of the BFR.

Several studies have investigated the photolytic degradation of DBDPE (Laouedj et al., 2014; Li et al., 2019a; Zhou et al., 2020) and photocatalysis of HBCDD (Li et al., 2019b; Zhou et al., 2014), mainly in organic solvents. Laouedj et al. (2014) have shown that DBDPE undergoes a stepwise reductive photolytic debromination in the solvent tetrahydrofuran (THF), which follows first-order kinetics. On the other hand, only a few works have investigated the photolysis of TTBPT. Lörchner et al. (2019) reported the photodegradation of TTBPT under UV (C) irradiation and sunlight, and their ability to identify, for the first time, the photoproducts from the photoconversion process of TTBPT in liquid medium.

In this study, a polymer matrix widely used in flame-retardant electrical appliances, electronic instruments and insulation materials (Grause et al., 2015), and HIPS was targeted. HIPS and thermoplastics such as ABS, PC and PP account for the majority of plastics in WEEE, with HIPS alone accounting for 25% (Charitopoulou et al., 2021). This composite material consists of a polystyrene phase and a dispersed polybutadiene rubber phase. In order to study the photodegradation of DBDE, HBCDD and novel brominated flame retardants (NBFRs), the determination of the degradation rate, the effect on the polymer matrix and the identification of the volatile products were carried out. Chemical structures of each considered BFRs are given in Figure 1. This study is a continuation of previously published work on the photodegradation of DBDE in ABS (Aldoori et al., 2020, 2023). The aim was to better understand the degradation process of brominated plastic waste by UV–visible irradiation and to optimise the experimental conditions. An alphabetical list of the abbreviations used and their meanings is given in Table 1.

**Table 1.** An alphabetical list of the abbreviations used and their meanings.

| Abbreviations  | Explications                                   |
|----------------|--|
| ABS            | Acrylonitrile butadiene styrene                |
| BDE            | Brominated diphenyl ether                      |
| BFR            | Brominated flame retardant                     |
| COP            | Conference of parties                          |
| DBDE           | Decabromodiphenyl ether                        |
| DBDPE          | Decabromodiphenyl ethane                       |
| DSC            | Differential scanning calorimetry              |
| EEE            | Electrical and electronic equipment            |
| EI             | Electron ionisation                            |
| FR             | Flame retardant                                |
| FTIR           | Fourier transform infrared spectroscopy        |
| HBCDD          | Hexabromocyclododecane                         |
| HIPS           | High impact polystyrene                        |
| HT             | High temperature                               |
| NBFRs          | Novel brominated flame retardants              |
| PBDEs          | Polybrominated diphenyl ethers                 |
| PBDF-OH        | Hydroxylated polybrominated dibenzofurans      |
| PC             | Polycarbonate                                  |
| POP            | Persistent organic pollutant                   |
| PP             | Polypropylene                                  |
| PS             | Polystyrene                                    |
| PTFE           | Polytetrafluoroethylene                        |
| QCM            | Quadrupole Mass Spectrometer                   |
| SC             | Stockholm convention                           |
| TBBP-A         | Tetrabromobisphenol-A                          |
| TGA            | Thermogravimetric analysis                     |
| THF            | Tetrahydrofuran                                |
| TTBPT          | Tris (tribromophenoxy)triazine                 |
| T <sub>g</sub> | Glass transition temperature                   |
| WEEE           | Waste from electrical and electronic equipment |

## Materials and methods

### Chemical products

Commercial DBDE (GC Deca 83) was purchased from Green-chemical S.p.a (Italy). Decabromodiphenyl ethane (DBDPE or FR-1410) and tris(tribromophenoxy)triazine (TTBPT or FR-245) were purchased from ICP-IP (Israel). Hexabromocyclododecane (HBCDD or SAYTEX BC-70HS) was purchased from Albemarle S.A. (Belgium), and HIPS styrolution<sup>®</sup> from INEOS Styrolution Group GmbH (Germany).

### Sample preparation

Blends of 90 wt% HIPS/10 wt% DBDE, 90 wt% HIPS/10 wt% DBDPE and 90 wt% HIPS/10 wt% TTBPT were prepared by extrusion at CREPIM (Bruay-la-Buissière, France). The 90 wt% HIPS/10 wt% HBCDD blend was prepared using a twin-screw micro-extruder (Xplore, Hannover, Germany). Thin films of 50 µm were produced using a Polystat 200T moulding press (Servitec Maschinenservice GmbH, Wustermark, Germany) under appropriate conditions of pressure (10–350 bar), temperature (230°C) and time (1–4 minutes) to achieve satisfactory homogeneity in all samples.

### Irradiation experiments

The irradiation of all the mixtures was carried out with a Xenon lamp LC8 (Hamamatsu Photonics France S.A.R.L., France), which covers a broad spectrum in the UV–visible range, similar to the spectrum of sunlight. This light source was equipped with an optical fibre with an outer beam diameter of 5 mm. The samples were fixed horizontally in a PTFE cell equipped with a quartz window of 1 mm thickness to allow maximum irradiance. The distance between the fibre and the sample was kept at 5 mm. The light intensity was determined to be 19 mW cm<sup>-2</sup> at a wavelength of 365 nm using a C6080-13 power meter (Hamamatsu Photonics France S.A.R.L., France).

## Physicochemical analysis

### Fourier transform infrared spectroscopy

Fourier transform infrared spectroscopy (FTIR) analysis was performed using a Perkin Elmer Frontier spectrometer (Perkin Elmer, Waltham, MA, USA). The films were analyzed in the transmission mode with the spectral range between 600 and 4000 cm<sup>-1</sup>. The number of cumulative scans was 16 with a spectral resolution of 4 cm<sup>-1</sup>. All spectra were baseline corrected and normalised to a polymer-specific band. The values of the BFR conversion rates (in%) were calculated using the expression  $(H_0 - H_t)/H_0 * 100$ , based on the absorbance of the band peaks at 1354 cm<sup>-1</sup> for DBDE and at 1245 cm<sup>-1</sup> for HBCDD.  $H_0$  and  $H_t$  correspond to the pristine and irradiated films, respectively, and  $H_t$  is given as function of irradiation time  $t$ .

In order to follow the evolution of the C–Br band of the DBDE molecule, the FTIR spectra of pristine and irradiated 90 wt% HIPS/10 wt% DBDE mixtures were obtained by using potassium bromide (KBr) pellets. The latter were prepared by grinding 3 mg of the sample and dispersing it in 97 mg of dry KBr powder. A pressure of 9 bar was applied during 3 minutes to prepare the KBr pellets.

### High-resolution two-step laser mass spectrometry

Identification of the presence and removal of BFR from plastic films was achieved using a high-resolution two-step laser mass spectrometer (Fasmatech S&T, Athens, Greece). The experimental setup is explained in detail elsewhere (Duca et al., 2021; Slavcinska et al., 2022). Briefly, the films were collected on a copper sample holder and introduced into the ion source of the mass spectrometer through a load-lock chamber. A neutral molecular plume was generated by laser desorption technique by second harmonic of Quantel Brilliant Nd:YAG laser (532 nm wavelength, 4 ns pulse duration, 10 Hz repetition rate). Desorbed neutral products were ionised by a second laser beam perpendicular to the plume (4th harmonic of a Quantel Brilliant Nd:YAG, 266 nm wavelength, 4 ns pulse duration, 10 Hz repetition rate). The ions produced were extracted in a differentially pumped octupole trap to be thermalised by collisions with helium

atoms injected by a fast solenoid valve. This increased the mass resolution of the spectrometer to  $m/\Delta m \sim 1.5 \times 10^4$ . The trapped ion packets were transported into the extraction/acceleration region of the orthogonal time-of-flight mass analyser. The mass spectra were recorded using nine mass windows to cover the 6–1200  $m/z$  mass range. For each mass spectrum, the signal generated by 35 cumulative laser pulses (fluence of 80–100  $\text{mJ cm}^{-2}$ ) at different positions on the film was averaged.

### Headspace- gas chromatography/mass spectrometry

The volatiles formed during irradiation were analysed by headspace gas chromatography/mass spectrometry (GC/MS). Samples of each mixture were cut into 1  $\text{cm}^2$  square pieces and irradiated vertically through an airtight Pyrex vial. Irradiation times were adjusted to match the photodegradation efficiency of the cell in relation to the light absorption of the glass vial. The vials were analysed immediately after irradiation using a headspace device coupled to a GC/MS system (HS-20, Perkin Elmer, Waltham, MA, USA). The oven temperature was set at 150°C to promote desorption from the vial walls and to avoid condensation. Volatile molecules were separated in a GC system (Clarus 680, Perkin Elmer, Waltham, MA, USA) using a 30 m  $\times$  0.25 mm Elite-XLB capillary column with a 0.10- $\mu\text{m}$  layer thickness and identified with a Quadrupole Mass Spectrometer (QMS) (Clarus 600T, Perkin Elmer, Waltham, MA, USA). The injector temperature was set at 180°C. Helium was used as the carrier gas at a constant pressure of 20 psi. Electron ionisation (EI) was performed at an energy of 70 eV, an ion source temperature of 180°C and an interface temperature of 300°C, scanning the range  $m/z=40\text{--}620$ . The initial programme temperature was set at 70°C for 3 minutes, followed by a ramp of 5°C  $\text{minute}^{-1}$  to 250°C. Identification was performed by matching the MS spectra of each molecule to a standard reference database from the National Institute of Standards and Technology (NIST), version NIST14. Experiments were repeated at least three times and only recurring molecules are listed.

### Thermogravimetric analysis

Thermogravimetric analysis (TGA) was performed on a Pyris 1 TGA apparatus (Perkin Elmer, Waltham, MA, USA) with a resolution of 1  $\mu\text{g}$ . The average sample mass was 8 mg, placed in Platinum-HT crucibles. Sample heating was performed from 25°C to 800°C with a rate of 10°C  $\text{minute}^{-1}$  under nitrogen atmosphere at a flow rate of 20  $\text{mL minute}^{-1}$ .

### Differential scanning calorimetry

The glass transition temperature of the polymers before and after irradiation was measured using a differential scanning calorimetry (DSC) 8000 instrument (Perkin Elmer, Waltham, MA, USA). Samples were prepared by placing 6–8 mg of polymers in sealed aluminium capsules. Three consecutive heating and cooling cycles were performed under nitrogen flow at a ramp rate of

10°C  $\text{minute}^{-1}$  in the temperature range from  $-75^\circ\text{C}$  to 190°C. The glass transition temperatures were calculated from the calorimetric data of the second heating ramp. The glass transition temperature was determined by the inflection point method using the Pyris TM Manager software (Perkin Elmer, Waltham, MA, USA).

## Results and discussion

### Determination of the degradation kinetics

The FTIR spectrum of pure DBDE is dominated by a broad, intense vibrational band located between 1250 and 1370  $\text{cm}^{-1}$ , as shown in Figure 2(a), which corresponds to the asymmetric stretching vibration of the C–O–C bridge connecting the two aromatic rings (Aldoori et al., 2020). Figure 2(b) presents a FTIR spectrum of irradiated pristine HIPS as well as spectra of non-irradiated pristine HIPS and 90 wt% HIPS/10 wt% DBDE samples. The latter shows a maximum at 1354  $\text{cm}^{-1}$  corresponding to the C–O–C vibration. This band largely exceeds a small

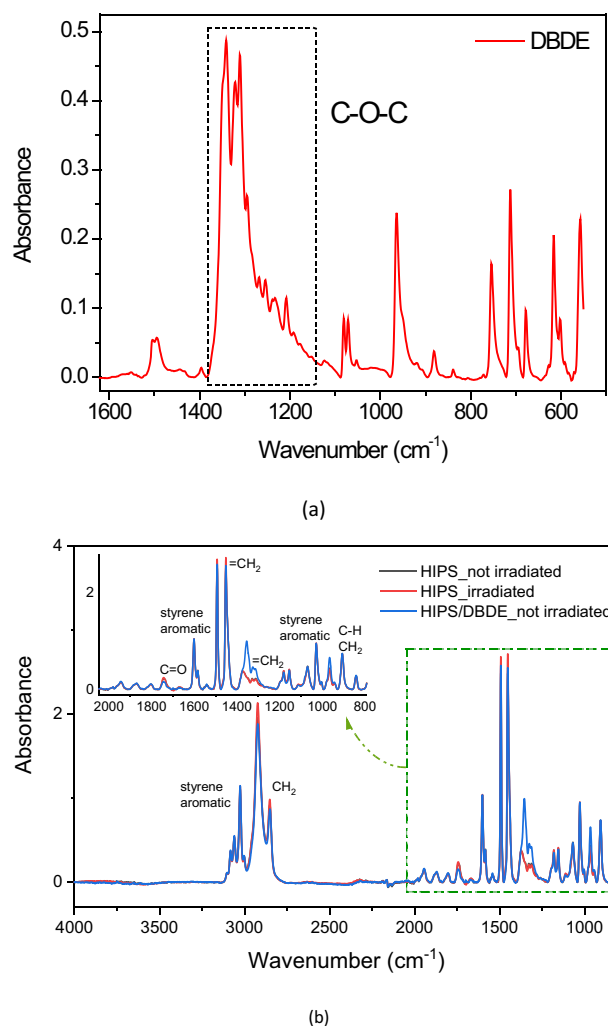


**Figure 2.** FTIR spectra of (a) DBDE in the 500–1600  $\text{cm}^{-1}$  spectral region, (b) non-irradiated 90 wt% HIPS/10 wt% DBDE as well as pristine HIPS before and after irradiation in the 800–4000  $\text{cm}^{-1}$  spectral region.

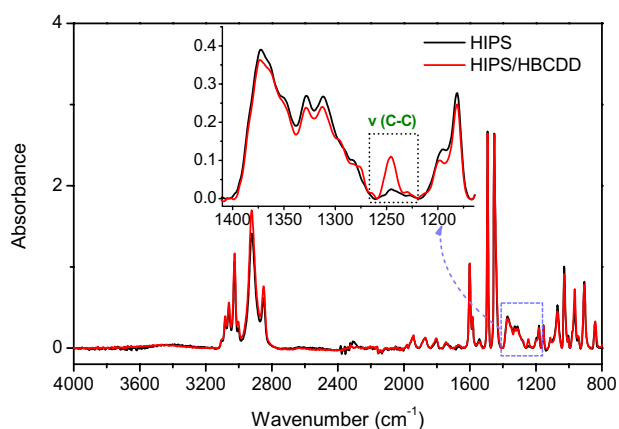
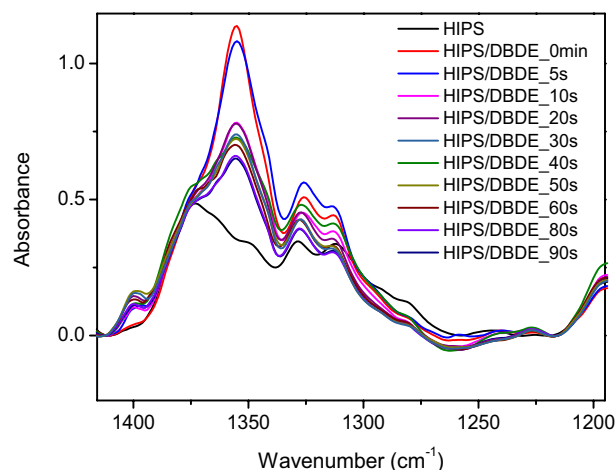


**Figure 3.** FTIR spectra of pristine HIPS and the non-irradiated 90wt% HIPS/10wt% HBCDD mixture, in the 4000–800  $\text{cm}^{-1}$  spectral region.

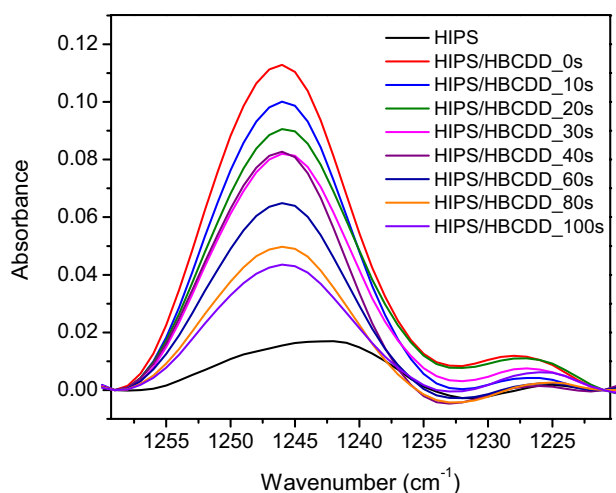
HIPS vibration band and has no overlapping effects with other HIPS bands (Al-Kadhemy et al., 2016; Liang and Krimm, 1958; Thanh Truc and Lee, 2017). It is important to note that the FTIR analysis of pristine HIPS irradiated under the same experimental conditions as the HIPS/BFR blend showed no spectral change compared to the pristine polymer.

As for HBCDD, the observation of the FTIR spectra of both systems: pristine HIPS and 90 wt% HIPS/10 wt% HBCDD mixture revealed the appearance of a new band located at 1245  $\text{cm}^{-1}$  for the latter, as shown in Figure 3. In fact, this band corresponds to the alicyclic C–C bond of the HBCDD molecule, which can be used as a signature (Zhang et al., 2014). The intensity of the two bands, C–O–C and alicyclic C–C, increase linearly with the concentration of BFR in the polymer matrix, thus allowing to follow the decrease of the concentration of brominated molecules after exposure to UV–visible radiation. The spectral evolution of the 90 wt% HIPS/10 wt% DBDE and 90 wt% HIPS/10 wt% HBCDD blends as a function of irradiation time are shown in Figure 4(a) and (b), respectively. A relatively strong reduction of the two bands corresponding to the ether bond and the alicyclic bond of DBDE and HBCDD molecules, respectively, was observed after a few seconds of exposure to UV–visible radiation. This is an indication of the degradation of the BFRs, resulting either in the cleavage of the C–Br bond, as suggested by its rather low dissociation energy, or in the cleavage of the C–O–C and C–C bonds, or both.

The two mixtures 90 wt% HIPS/10 wt% DBDE and 90 wt% HIPS/10 wt% HBCDD, as well as pristine HIPS, showed rather similar FTIR spectra, except for the presence of the two characteristic bands C–O–C and acyclic C–C. These bands are specific for the brominated molecules DBDE and HBCDD and are located at 1354 and 1254  $\text{cm}^{-1}$ , respectively. As a result, the C–Br vibrations of DBDE (960, 761 and 615  $\text{cm}^{-1}$ ) and HBCDD (500–700  $\text{cm}^{-1}$ ) were difficult to detect. In fact, they represent weak signals and overlap with the intense bands of the polymer. However, in the case of the 90 wt% HIPS/10 wt% DBDE blend, a shoulder at 615  $\text{cm}^{-1}$  was observed within a broad peak ranging from 605 to 640  $\text{cm}^{-1}$  (Figure 5). The intensity of this shoulder is



(a)



(b)

**Figure 4.** Evolution of the FTIR spectra of 50- $\mu\text{m}$  thick films of the mixtures (a) 90wt% HIPS/10wt% DBDE and (b) 90wt% HIPS/10wt% HBCDD, during irradiation in ambient air.

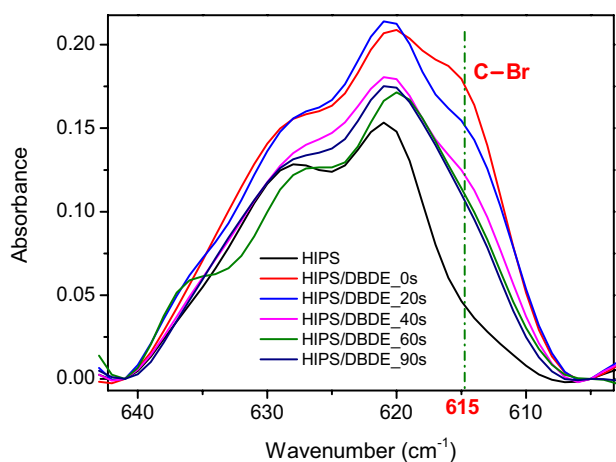
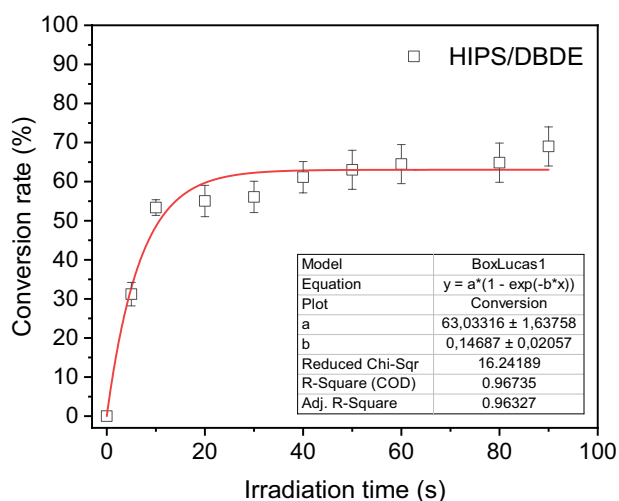
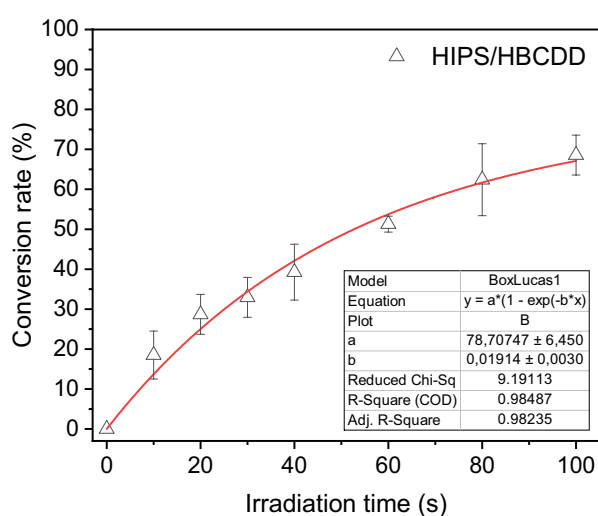


**Figure 5.** Evolution of the FTIR spectra of 50  $\mu\text{m}$  thick films of the 90wt% HIPS/10wt% DBDE blend at 615  $\text{cm}^{-1}$  during irradiation in ambient air.



(a)



(b)

**Figure 6.** Photodegradation kinetics in ambient air of the mixtures (a) 90 wt% HIPS/10 wt% DBDE, (b) 90 wt% HIPS/10 wt% HBCDD, based on the absorbance of the band peaks at  $1354\text{ cm}^{-1}$  for DBDE and at  $1245\text{ cm}^{-1}$  for HBCDD.

too low to reliably monitor the presence of bromine in the polymer matrix. However, a decrease in the shoulder as a function of exposure time was observed, consistent with the decrease in the main C–O–C band of DBDE.

The effect of UV–vis irradiation was compared for the two systems 90 wt% HIPS/10 wt% BFR and pristine HIPS, according to the decrease of the absorption band at  $1354\text{ cm}^{-1}$  for DBDE and at  $1245\text{ cm}^{-1}$  for HBCDD. The results obtained after calculating the BFR conversions using the above formula are shown in Figure 6(a) and (b). It should be noted that this approach provides only a rough estimate of the BFR conversion, as the absorption band considered here could be subject to overlapping effects with other bands, especially as the photolysis progresses. The photodegradation of DBDE and HBCDD followed pseudo-first-order kinetics with a rate constant of  $0.14$  and  $0.019\text{ s}^{-1}$ , respectively,

with a degradation rate of more than 50%. The degradation rate varies considerably depending on the characteristics of the solids and different irradiation conditions (Pan et al., 2016). HIPS is sensitive to UV–visible radiation in the presence of bromine radicals and in the presence of atmospheric oxygen (David et al., 1977). The latter authors reported that the polymer underwent embrittlement, reflected by yellowing of the film surface, which slowed the degradation of the BFRs by hindering radiation penetration. As a result, films of the 90 wt% HIPS/10 wt% HBCDD blend were photo-oxidised before reaching a plateau, thus preventing photodegradation tracking at longer exposure times.

### Efficiency of the debromination process

Two-step laser mass spectrometry mass spectra were recorded in negative ion mode to illustrate the bromine removal obtained after UV–vis irradiation of films composed of 90 wt% HIPS and 10 wt% BFRs. The mass spectra of these blends before and after irradiation were compared with the spectra of pure pristine HIPS. Figure 7(a) and (b) shows the results obtained for 90 wt% HIPS/10 wt% DBDE and 90 wt% HIPS/10 wt% HBCDD, respectively. The peaks observed at 79 and 81 m/z in both HIPS/BFR mixtures, which are not seen in pristine HIPS, correspond well to the fragmented bromide. The additional high intensity peaks detected in all spectra at 60, 72, 84 and 96 m/z were attributed to enriched carbon clusters C5, C6, C7 and C8, respectively, and associated with pristine HIPS. In both HIPS/BFR systems, the intensity of the bromide peaks decreased by one order of magnitude after 90 s (HIPS/DBDE) and 100 s (HIPS/HBCDD) UV–vis irradiation, confirming the efficiency of the debromination process.

### Identification of volatile products

Detection and identification of volatile by-products were performed using a headspace instrument coupled to GC/MS analysis, which revealed the presence of several brominated as well as non-brominated molecules listed in Table 2, for the mixtures 90 wt% HIPS/10 wt% DBDE, 90 wt% HIPS/10 wt% DBDPE and 90 wt% HIPS/10 wt% TTBPT. The corresponding GC chromatograms are shown in Figure 8(a)–(c), respectively.

Khaled et al. (2018b) reported the presence of several photoproducts in the gas phase, that are commonly detected during the oxidation of PS. These were carboxylic acids such as formic acid, malonic acid and benzoic acid. These products were not detected for the 90 wt% HIPS/10 wt% DBDE and 90 wt% HIPS/10 wt% DBDPE blends. However, only benzoic acid was identified for the 90 wt% HIPS/10 wt% TTBPT mixture. On the other hand, several photoproducts in the form of aromatic compounds could be detected upon irradiation of HIPS/BFR. These brominated molecules should originate from the combination of released brominated radicals with volatile monomers and small polymer fragments. This confirms that bromine radicals released during irradiation do attack polymer chains to form volatile brominated molecules that could accelerate plastic degradation.

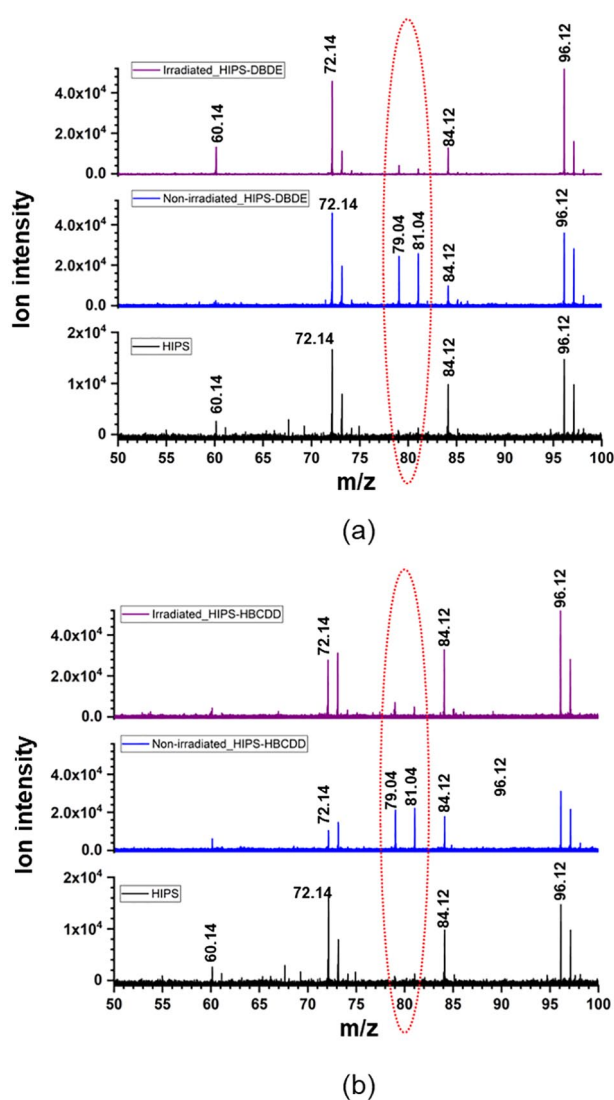


**Figure 7.** (a) Comparison of the HR-L2MS spectra of pristine HIPS (black colour), non-irradiated (blue colour) and an irradiated (90 s) mixture of 90 wt% HIPS/10 wt% DBDE (purple colour). (b) Comparison of HR-L2MS spectra of pristine HIPS (black colour), non-irradiated (blue colour) and an irradiated (100 s) mixture of 90 wt% HIPS/10 wt% HBCDD (purple colour).

In fact, no volatile by-products were detected during irradiation of the virgin polymer.

Styrene monomers were identified in the three mixtures 90 wt% HIPS/10 wt% DBDE, 90 wt% HIPS/10 wt% DBDPE and 90 wt% HIPS/10 wt% TTBPT because bromine radicals from the phototransformation of BFRs react with HIPS in the presence of atmospheric oxygen. The low molecular weight species of DBDE and DBDPE could then combine with these monomers to form brominated species such as (1,2-dibromoethyl) benzene, (1-bromoethyl)benzene, dibromoethylbenzene and bromoethylbenzene. These species could also be formed from the fragments produced by cleavage of the ether bond in the case of DBDE or the ethane bridge in the case of DBDPE. Bromononane could also be formed from butadiene dimers or from cleavage of the polymer chain.

In the case of TTBPT, the main by-products were bromophenols, which were most likely formed from the flame retardant itself by cleavage of an ether bond, independent of interaction with the polymer matrix. These small molecules contained less bromine than the original molecule.

For comparison, Koch et al. (2016, 2019) studied the photo-degradation of a new BFR called polymer FR, a block copolymer of polystyrene and brominated polybutadiene. The latter was immersed in water to trap the degradation by-products. Indeed, they found a certain solubility of these products in water and several brominated molecules were detected. Their chemical structures were similar to those of the by-products identified above, but with a higher bromine density.

### Evaluation of thermal properties

In amorphous polymeric materials, the glass transition temperature is specifically related to the mobility of the polymer chains and determines the transition between the glassy and rubbery polymer states (Vilaplana et al., 2007). The results of the DSC analysis of the 90 wt% HIPS/10 wt% DBDE blend, shown in Figure 9, showed no increase in the glass transition temperature ( $T_g$ ) of pristine HIPS after irradiation. Neither endo- nor exothermic phenomena other than those related to  $T_g$  were observed in the temperature range studied ( $-75^\circ\text{C}$  to  $190^\circ\text{C}$ ). Prior to irradiation treatment, the  $T_g$  of the 90 wt% HIPS/10 wt% DBDE mixture was determined to be about  $93.3^\circ\text{C}$ . The decrease from the corresponding value of pristine HIPS ( $96.4^\circ\text{C}$ ) was attributed to the impurity effect caused by the addition of DBDE, which increased the mobility of the polymer chains. For the polybutadiene portion in HIPS, the corresponding glass transition was expected to occur at low temperatures around  $-90^\circ\text{C}$  (He et al., 1986), which was not detected in this report.

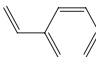
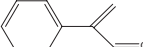
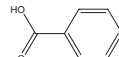
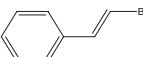
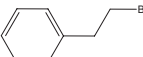
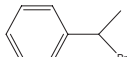
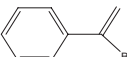
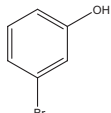
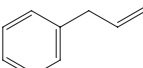
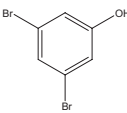
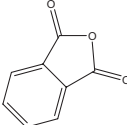
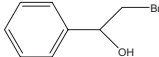
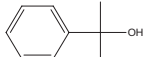
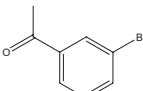
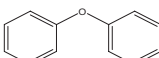
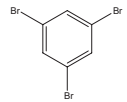
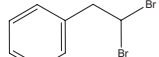
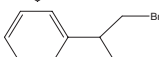
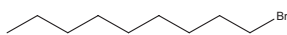
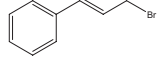
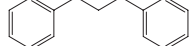
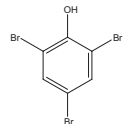
On the other hand, in the case of irradiated 90 wt% HIPS/10 wt% DBDE, the  $T_g$  increased and reached the value of  $101^\circ\text{C}$ . This increase may be related to the presence of a certain amount of cross-linked species. Another explanation is a decrease in molecular mobility due to the modification of the sample surface by an oxidation phenomenon that modifies the free volume. However, this increase in  $T_g$  remained moderate.

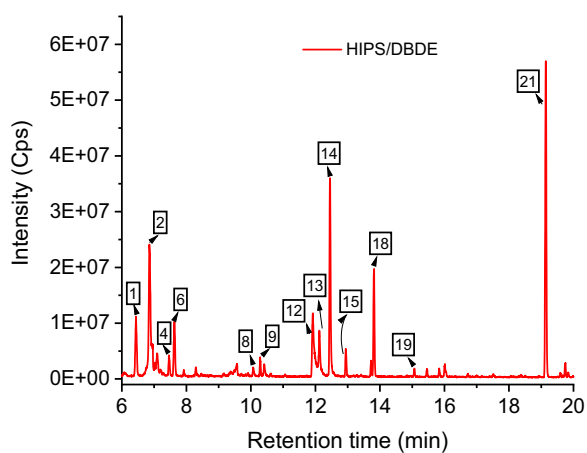
Thermograms and their derivatives obtained by TGA of pristine HIPS and the 90 wt% HIPS/10 wt% BFR blend are shown in Figure 10. HIPS showed complete degradation in a single step. Mass loss started at about  $200^\circ\text{C}$ , and the entire polymer was degraded at  $450^\circ\text{C}$ . The 90 wt% HIPS/10 wt% DBDE, 90 wt% HIPS/10 wt% DBDPE and 90 wt% HIPS/10 wt% TTBPT blends degraded in two steps: The thermograms (Figure 10(a) and (b)) show a major mass loss of 96% between about  $250^\circ\text{C}$  and  $445^\circ\text{C}$ , corresponding to both the polymer and the added BFRs. This mass loss was followed by another step up to  $520^\circ\text{C}$ , related to partial crosslinking of the polymer, as shown by the derivatives shown in Figure 10(c) and (d).

For the 90 wt% HIPS/10 wt% HBCDD blends, three degradation steps were observed. The HBCDD degraded first between

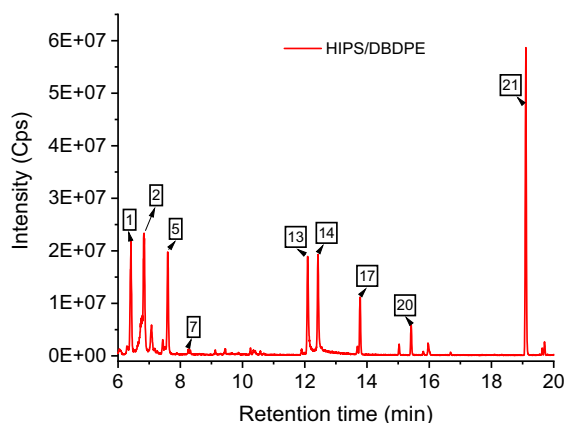


**Table 2.** Representation of the identified molecules in the gas phase for the mixtures (a) 90wt% HIPS/10wt% DBDE, (b) 90wt% HIPS/10wt% DBDPE and (c) 90wt% HIPS/10wt% TTBPT after the end of the irradiation process.

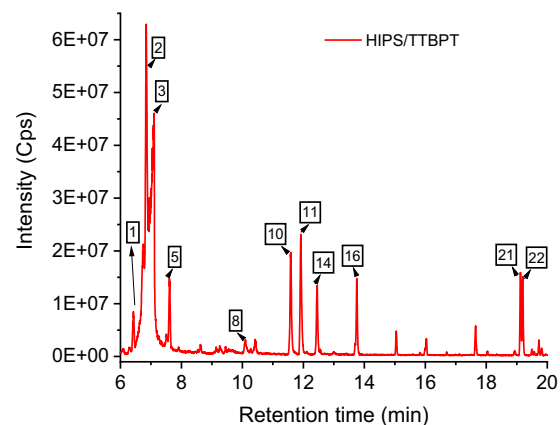
| No. | Molecules identified by MS   | CAS number | Chemical structure  | HIPS/DBDE | HIPS/DBDPE | HIPS/TTBPT |
|-----|------------------------------|------------|---|-----------|------------|------------|
| 1   | Styrene                      | 9003-53-6  |    | X         | X          | X          |
| 2   | 2-Phenylpropenal             | 495-10-3   |    | X         | X          | X          |
| 3   | Benzoic acid                 | 65-85-0    |    |           |            | X          |
| 4   | 2-Bromovinylbenzene          | 588-72-7   |    | X         |            |            |
| 5   | Bromoethylbenzene            | 103-63-9   |    |           | X          | X          |
| 6   | (1-Bromoethyl) benzene       | 585-71-7   |    | X         |            |            |
| 7   | (1-Bromoethenyl) benzene     | 98-81-7    |    |           | X          |            |
| 8   | Bromophenol                  | 591-20-8   |    | X         |            | X          |
| 9   | 2-Propenylbenzene            | 300-57-2   |    | X         |            |            |
| 10  | Dibromophenol                | 626-41-5   |   |           |            | X          |
| 11  | Phthalic anhydride           | 85-44-9    |  |           |            | X          |
| 12  | 2-Bromo-1-phenylethanol      | 2425-28-7  |  | X         |            |            |
| 13  | 2-Phenyl-2-propanol          | 617-94-7   |  | X         | X          |            |
| 14  | Bromophenylethenone          | 2142-63-4  |  | X         | X          | X          |
| 15  | Diphenyl ether               | 101-84-8   |  | X         |            |            |
| 16  | Tribromobenzene              | 626-39-1   |  |           |            | X          |
| 17  | 1,[2,2-Dibromoethyl] benzene | 30812-87-4 |  |           | X          |            |
| 18  | 1,[1,2-Dibromoethyl] benzene | 93-52-7    |  | X         |            |            |
| 19  | Bromononane                  | 693-58-3   |  | X         |            |            |
| 20  | 3-Bromo-1-phenyl-1-propene   | 4392-24-9  |  |           | X          |            |
| 21  | 1,3-Diphenylpropane          | 1081-75-0  |  | X         | X          | X          |
| 22  | 2,4,6-Tribromophenol         | 118-79-6   |  |           |            | X          |



(a)



(b)



(c)

**Figure 8.** GC chromatograms of mixtures (a) 90 wt% HIPS/10 wt% DBDE, (b) 90 wt% HIPS/10 wt% DBDPE and (c) 90 wt% HIPS/10 wt% TTBPT, after irradiation. Peak labels refer to the list in Table 2 for each blend.

200°C and 300°C (Barontini et al., 2001) with a mass loss of 9.3%, followed by a second mass loss of 86.7% corresponding to the degradation of the polymer backbone. The thermal degradation products of HBCDD reacted with the polymer during heating to form a thermally resistant fraction (Figure 10(b)). However, the latter was completely degraded between 430°C and 520°C (Figure 10(d)).

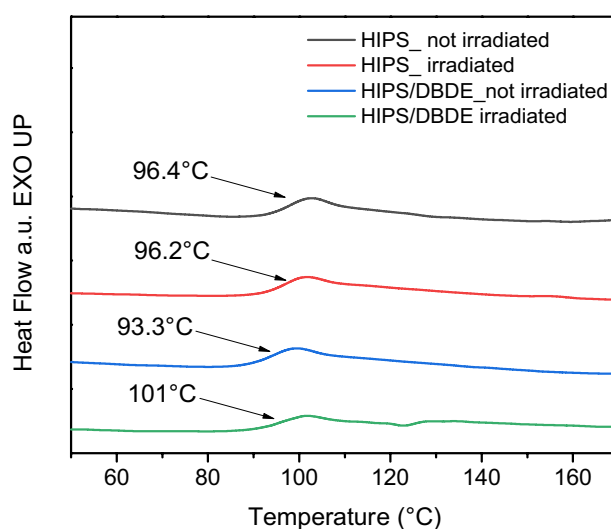


**Figure 9.** Heat flow in arbitrary units from DSC measurements of the HIPS polymer film [0 wt% DBDE] and the 90 wt% HIPS/10 wt% DBDE blend before and after irradiation.

The thermal behaviour of all 90 wt% HIPS/10 wt% BFR blends was also investigated after irradiation. A slight increase in the onset temperature of degradation was observed for the three irradiated 90 wt% HIPS/10 wt% DBDE, 90 wt% HIPS/10 wt% TTBPT and 90 wt% HIPS/10 wt% HBCDD blends (Figure 10(a) and (b)). This could be an indication of thermal degradation of the BFRs. The increase was more interesting in the case of the 90 wt% HIPS/10 wt% HBCDD mixture because it occurred in the temperature range of HBCDD degradation, recording a mass loss of 6.6%. The derivative of the 90 wt% HIPS/10 wt% DBDPE blend (Figure 10(d)) showed a slight shift to lower temperatures with respect to the polymer.

Finally, a small increase in the heat resistant fraction was also observed for the mixtures 90 wt% HIPS/10 wt% DBDE and 90 wt% HIPS/10 wt% TTBPT. This could be due to photoproducts resulting from irradiation. However, the degradation profiles were globally quite similar for all samples, and no formation of carbonaceous residues was observed.

## Conclusions

In this report, the photodegradation of dispersions of DBDE, HBCDD and the NBRs DBDPE and TTBPT in HIPS was investigated by FTIR and L2MS. HIPS was chosen as the polymer matrix because it contributes to the main plastic fractions of WEEE. The photodegradation of DBDE and HBCDD was found to follow pseudo-first-order kinetics with a rate constant of 0.14 and 0.019 s<sup>-1</sup>, respectively. The overall decontamination of both brominated systems, DBDE/HIPS and HBCDD/HIPS, was significant (>50%).

Identification of volatile by-products released during irradiation of DBDE, DBDPE and TTBPT containing HIPS showed that brominated aromatic compounds were present in all irradiated samples, among which bromophenols were the

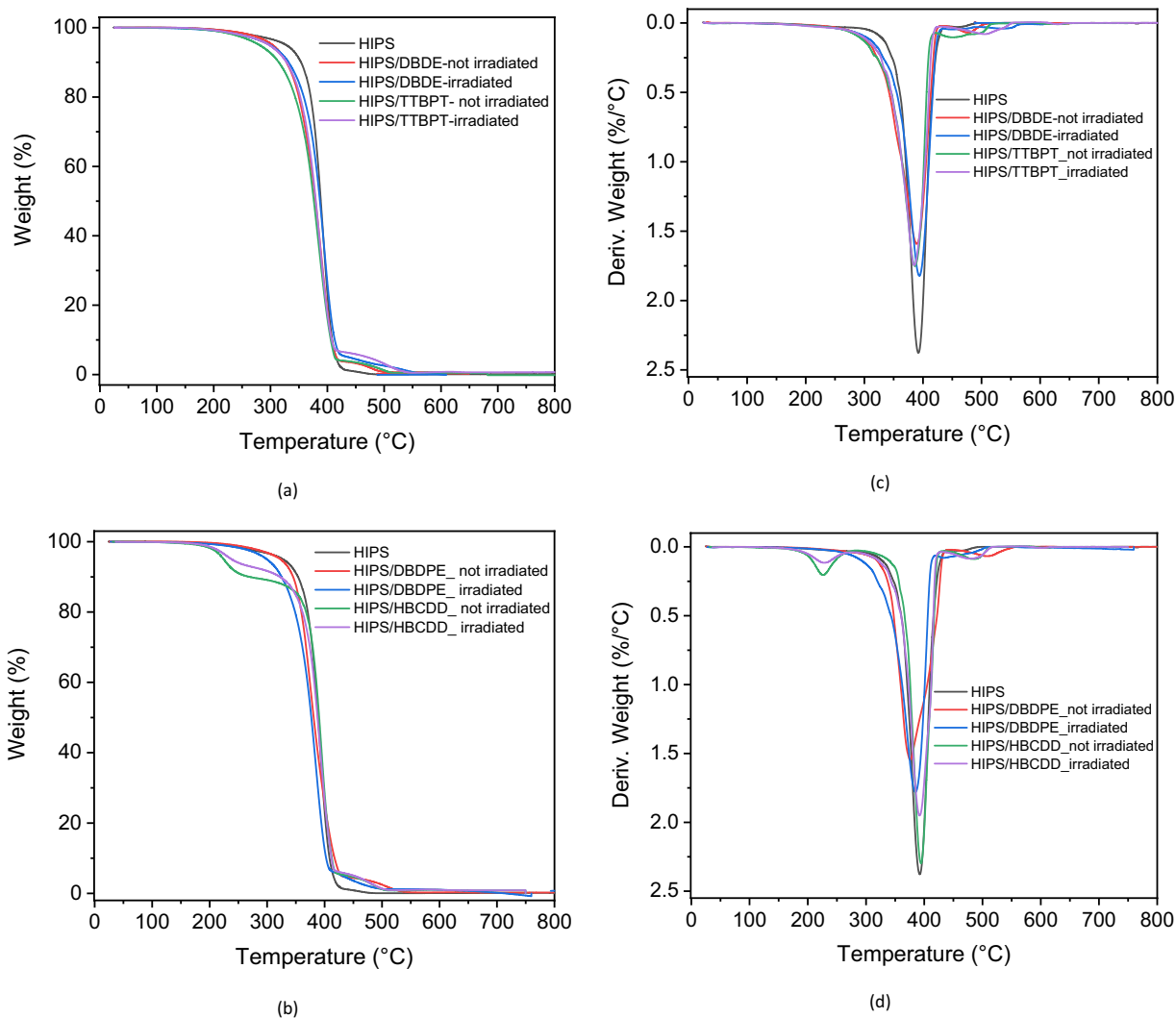


**Figure 10.** (a, b) TGA thermograms and (c, d) their derivatives for HIPS polymer (0wt% DBDE) and for 90wt% HIPS/10wt% DBDE, 90wt% HIPS/10wt% DBDPE, 90wt% HIPS/10wt% TTBPT and 90wt% HIPS/10wt% HBCDD blends, before and after irradiation.

most abundant species in the case of TTBPT molecule. The results obtained showed a degradation of the exposed sample surface during the photolytic process, related to cross-linking effects due to the presence of bromine radicals. However, the thermal properties of HIPS were globally preserved. UV-visible irradiation was shown to be an effective and simple method to destroy BFRs dispersed in HIPS, thus allowing the reuse of the decontaminated HIPS for further processing. Further research will be conducted to evaluate the toxicity of the volatile by-products generated during photolysis.

### Acknowledgements

All authors would like to thank French funding agency ANR for financial support, in the framework of the EffPhoB project (2021–2025). Some of the authors, HO, HA, ZB, CF, PS and UM, members of the Valbree project (2018–2022), gratefully acknowledge the financial support from the corresponding funding agencies. These authors would like to express their gratitude to the technical teams from France, Wallonie and Vlaanderen regions of the Interreg FWVL V programme.

### Declaration of conflicting interests

The authors declared no potential conflicts of interest with respect to the research, authorship, and/or publication of this article.

### Funding

The authors received no financial support for the research, authorship, and/or publication of this article.

### ORCID iDs

Venkateswara Rao Mundlapati  <https://orcid.org/0000-0003-0559-9684>

Philippe Supiot  <https://orcid.org/0000-0003-0352-6422>

Yvain Carpentier  <https://orcid.org/0000-0002-1677-4874>

Ulrich Maschke  <https://orcid.org/0000-0001-7970-1966>

### References

Alaee M (2003) An overview of commercially used brominated flame retardants, their applications, their use patterns in different countries/regions and possible modes of release. *Environment International* 29: 683–689.

- Aldoori H, Bouberka Z, Feuchter H, et al. (2023) Recycling of plastics from e-waste via photodegradation in a low-pressure reactor: The case of decabromodiphenyl ether dispersed in poly(acrylonitrile-butadiene-styrene) and poly(carbonate). *Molecules* 28: 2491.
- Aldoori H, Bouberka Z, Nadim A, et al. (2020) Photodegradation of decabromo diphenyl ether flame retardant in poly (acrylonitrile butadiene styrene) (ABS). *Journal of Macromolecular Science, Part B* 59: 609–620.
- Al-Kadhemy MFH, Rasheed ZS and Salim SR (2016) Fourier transform infrared spectroscopy for irradiation coumarin doped polystyrene polymer films by alpha ray. *Journal of Radiation Research and Applied Sciences* 9: 321–331.
- Barontini F, Cozzani V and Petarca L (2001) Thermal stability and decomposition products of hexabromocyclododecane. *Industrial & Engineering Chemistry Research* 40: 3270–3280.
- Baumgartner R, Stieger GK and McNeill K (2013) Complete hydrodehalogenation of polyfluorinated and other polyhalogenated benzenes under mild catalytic conditions. *Environmental Science & Technology* 47: 6545–6553.
- Charitopoulou MA, Kalogiannis KG, Lappas AA, et al. (2021) Novel trends in the thermo-chemical recycling of plastics from WEEE containing brominated flame retardants. *Environmental Science and Pollution Research* 28: 59190–59213.
- Christiansson A, Eriksson J, Teclechiel D, et al. (2009) Identification and quantification of products formed via photolysis of decabromodiphenyl ether. *Environmental Science and Pollution Research* 16: 312–321.
- Couderc M, Poirier L, Zalouk-Vergnoux A, et al. (2015) Occurrence of POPs and other persistent organic contaminants in the European eel (*Anguilla anguilla*) from the Loire estuary, France. *Science of the Total Environment* 505: 199–215.
- Covaci A, Voorspoels S and de Boer J (2003) Determination of brominated flame retardants, with emphasis on polybrominated diphenyl ethers (PBDEs) in environmental and human samples – A review. *Environment International* 29: 735–756.
- Currier HA, Fremlin KM, Elliott JE, et al. (2020) Bioaccumulation and biomagnification of PBDEs in a terrestrial food chain at an urban landfill. *Chemosphere* 238: 124577.
- David C, Baeyens-Volant D, Delaunois G, et al. (1977) Photo-oxidation of polymers – III. *European Polymer Journal* 14: 501–507.
- Drage DS, Heffernan AL, Cunningham TK, et al. (2019) Serum measures of hexabromocyclododecane (HBCDD) and polybrominated diphenyl ethers (PBDEs) in reproductive-aged women in the United Kingdom. *Environmental Research* 177: 108631.
- Duca D, Rahman M, Carpentier Y, et al. (2021) Chemical characterization of size-selected nanoparticles emitted by a gasoline direct injection engine: Impact of a catalytic stripper. *Fuel* 294: 120317.
- Eriksson J, Green N, Marsh G, et al. (2004a) Photochemical decomposition of 15 polybrominated diphenyl ether congeners in methanol/water. *Environmental Science & Technology* 38: 3119–3125.
- Eriksson J, Rahm S, Green N, et al. (2004b) Photochemical transformations of tetrabromobisphenol A and related phenols in water. *Chemosphere* 54: 117–126.
- Gherdaoui CE, Bouberka Z, Supiot P, et al. (2021) Method for dechlorination of one or more aromatic organochlorine compound(s) contained in an oil or forming said oil – associated electrical/electronic device and installation. *European Publication Server* EP3881907: 1–48. Available at: [https://data.epo.org/publication-server/document?iDocId=6643418&iFoRmat=0&fbclid=IwAR2VsNwuZLvDt2IWUT29FmyQomxZW0y3bGVwf\\_V7IUc49wNU9ANVNKk7WyM](https://data.epo.org/publication-server/document?iDocId=6643418&iFoRmat=0&fbclid=IwAR2VsNwuZLvDt2IWUT29FmyQomxZW0y3bGVwf_V7IUc49wNU9ANVNKk7WyM) (accessed 28 July 2023).
- Grause G, Fonseca JD, Tanaka H, et al. (2015) A novel process for the removal of bromine from styrene polymers containing brominated flame retardant. *Polymer Degradation and Stability* 112: 86–93.
- Guo J, Stubbings WA, Romanak K, et al. (2018) Alternative flame retardant, 2,4,6-tris(2,4,6-tribromophenoxy)-1,3,5-triazine, in an e-waste recycling facility and house dust in North America. *Environmental Science & Technology* 52: 3599–3607.
- He C, Wang X, Thai P, et al. (2018) Organophosphate and brominated flame retardants in Australian indoor environments: Levels, sources, and preliminary assessment of human exposure. *Environmental Pollution* 235: 670–679.
- He T, Li B and Ren S (1986) Glass transition temperature and chain flexibility of 1,2-polybutadiene. *Journal of Applied Polymer Science* 31: 873–884.
- Hennebert P and Filella M (2018) WEEE plastic sorting for bromine essential to enforce EU regulation. *Waste Management* 71: 390–399.
- Hou R, Lin L, Li H, et al. (2021) Occurrence, bioaccumulation, fate, and risk assessment of novel brominated flame retardants (NBFRs) in aquatic environments – A critical review. *Water Research* 198: 117168.
- Kajiwaru N, Desborough J, Harrad S, et al. (2013) Photolysis of brominated flame retardants in textiles exposed to natural sunlight. *Environmental Science: Processes & Impacts* 15: 653–660.
- Kajiwaru N, Noma Y and Takigami H (2008) Photolysis studies of technical decabromodiphenyl ether (DecaBDE) and ethane (DeBDethane) in plastics under natural sunlight. *Environmental Science & Technology* 42: 4404–4409.
- Khaled A, Richard C, Rivaton A, et al. (2018a) Photodegradation of brominated flame retardants in polystyrene: Quantum yields, products and influencing factors. *Chemosphere* 211: 943–951.
- Khaled A, Rivaton A, Richard C, et al. (2018b) Phototransformation of plastic containing brominated flame retardants: Enhanced fragmentation and release of photoproducts to water and air. *Environmental Science & Technology* 52: 11123–11131.
- Klinčić D, Dvorščak M, Jagić K, et al. (2020) Levels and distribution of polybrominated diphenyl ethers in humans and environmental compartments: A comprehensive review of the last five years of research. *Environmental Science and Pollution Research* 27: 5744–5758.
- Koch C, Dundua A, Aragon-Gomez J, et al. (2016) Degradation of polymeric brominated flame retardants: Development of an analytical approach using PolyFR and UV irradiation. *Environmental Science & Technology* 50: 12912–12920.
- Koch C, Nachev M, Klein J, et al. (2019) Degradation of the polymeric brominated flame retardant “Polymeric FR” by heat and UV exposure. *Environmental Science & Technology* 53: 1453–1462.
- Koch C, Schmidt-Kötters T, Rupp R, et al. (2015) Review of hexabromocyclododecane (HBCD) with a focus on legislation and recent publications concerning toxicokinetics and -dynamics. *Environmental Pollution* 199: 26–34.
- Laouedj N, Elaziouti A, Maschke U, et al. (2014) Spectroscopic behavior of Saytex 8010 under UV-visible light and comparative thermal study with some flame bromine retardant. *Journal of Photochemistry and Photobiology A: Chemistry* 275: 96–102.
- Li B, Shi J, Zhang J, et al. (2023) Occurrence and ecological risk assessment of 2,2',4,4'-tetrabromodiphenyl ether and decabromodiphenyl ether in surface waters across China. *Chemosphere* 312: 137215.
- Li C, Zuo J, Liang S, et al. (2019a) Photodegradation of decabromodiphenyl ethane (DBDPE) adsorbed on silica gel in aqueous solution: Kinetics, products, and theoretical calculations. *Chemical Engineering Journal* 375: 121918.
- Li Q, Wang L, Fang X, et al. (2019b) Synergistic effect of photocatalytic degradation of hexabromocyclododecane in water by UV/TiO<sub>2</sub>/persulfate. *Catalysts* 9: 189.
- Liang CY and Krimm S (1958) Infrared spectra of high polymers. VI. Polystyrene. *Journal of Polymer Science* 27: 241–254.
- Ling S, Lu C, Fu M, et al. (2022) Distribution characteristics and risks assessment of brominated flame retardants in surface soil from both a legacy and a new e-waste dismantling site. *Journal of Cleaner Production* 373: 133970.
- Lörchner D, Kraus W and Köppen R (2019) Photodegradation of the novel brominated flame retardant 2,4,6-tris-(2,4,6-tribromophenoxy)-1,3,5-triazine in solvent system: Kinetics, photolysis products and pathway. *Chemosphere* 229: 77–85.
- Morris S, Allchin CR, Zegers BN, et al. (2004) Distribution and fate of HBCD and TBBPA brominated flame retardants in North Sea estuaries and aquatic food webs. *Environmental Science & Technology* 38: 5497–5504.
- Pan Y, Tsang DCW, Wang Y, et al. (2016) The photodegradation of polybrominated diphenyl ethers (PBDEs) in various environmental matrices: Kinetics and mechanisms. *Chemical Engineering Journal* 297: 74–96.
- Panda D, Sethu V and Manickam S (2020) Removal of hexabromocyclododecane using ultrasound-based advanced oxidation process: Kinetics, pathways and influencing factors. *Environmental Technology & Innovation* 17: 100605.
- Pietroń WJ and Małagocki P (2017) Quantification of polybrominated diphenyl ethers (PBDEs) in food. A review. *Talanta* 167: 411–427.
- Saeed A, Altaraneh M, Siddique K, et al. (2020) Photodecomposition properties of brominated flame retardants (BFRs). *Ecotoxicology and Environmental Safety* 192: 110272.

- Slavicinska K, Duca D, Egorov D, et al. (2022) Link between polycyclic aromatic hydrocarbon size and aqueous alteration in carbonaceous chondrites revealed by laser mass spectrometry. *ACS Earth and Space Chemistry* 6: 1413–1428.
- Sühling R, Möller A, Freese M, et al. (2013) Brominated flame retardants and dechloranes in eels from German Rivers. *Chemosphere* 90: 118–124.
- Taurino R, Pozzi P and Zanasi T (2010) Facile characterization of polymer fractions from waste electrical and electronic equipment (WEEE) for mechanical recycling. *Waste Management* 30: 2601–2607.
- Thanh Truc NT and Lee B-K (2017) Combining ZnO/microwave treatment for changing wettability of WEEE styrene plastics (ABS and HIPS) and their selective separation by froth flotation. *Applied Surface Science* 420: 746–752.
- Touaa ND, Bouberka Z, Gherdaoui CE, et al. (2020) Titanium and iron-modified delaminated muscovite as photocatalyst for enhanced degradation of tetrabromobisphenol A by visible light. *Functional Materials Letters* 13: 2051008.
- Vilaplana F, Ribes-Greus A and Karlsson S (2007) Analytical strategies for the quality assessment of recycled high-impact polystyrene: A combination of thermal analysis, vibrational spectroscopy, and chromatography. *Analytica Chimica Acta* 604: 18–28.
- Wäger PA, Schluep M, Müller E, et al. (2012) RoHS regulated substances in mixed plastics from waste electrical and electronic equipment. *Environmental Science & Technology* 46: 628–635.
- Waiyarat S, Boontanon SK, Boontanon N, et al. (2022) Concentrations and human exposure to hexabromocyclododecane and tetrabromobisphenol A from the indoor environment in Bangkok metropolitan area, Thailand. *Journal of Environmental Exposure Assessment* 1: 11.
- Wang C, Zeng L, Li Y, et al. (2022) Decabromodiphenyl ethane induces locomotion neurotoxicity and potential Alzheimer's disease risks through intensifying amyloid-beta deposition by inhibiting transthyretin/transthyretin-like proteins. *Environment International* 168: 107482.
- Wang X, Ling S, Guan K, et al. (2019) Bioconcentration, biotransformation, and thyroid endocrine disruption of decabromodiphenyl ethane (DBDPE), a novel brominated flame retardant, in Zebrafish Larvae. *Environmental Science & Technology* 53: 8437–8446.
- Wu J, Zhang Y, Luo X, et al. (2012) A review of polybrominated diphenyl ethers and alternative brominated flame retardants in wildlife from China: Levels, trends, and bioaccumulation characteristics. *Journal of Environmental Sciences* 24: 183–194.
- Zhang K, Huang J, Wang H, et al. (2014) Mechanochemical degradation of hexabromocyclododecane and approaches for the remediation of its contaminated soil. *Chemosphere* 116: 40–45.
- Zhou D, Wu Y, Feng X, et al. (2014) Photodegradation of hexabromocyclododecane (HBCD) by Fe(III) complexes/H<sub>2</sub>O<sub>2</sub> under simulated sunlight. *Environmental Science and Pollution Research* 21: 6228–6233.
- Zhou D, Zheng X, Liu X, et al. (2020) Photodegradation of 1,3,5-tris-(2,3-dibromopropyl)-1,3,5-triazine-2,4,6-trione and decabromodiphenyl ethane flame retardants: Kinetics, main products, and environmental implications. *Journal of Hazardous Materials* 398: 122983.
- Zuiderveen EAR, Slootweg JC and de Boer J (2020) Novel brominated flame retardants – A review of their occurrence in indoor air, dust, consumer goods and food. *Chemosphere* 255: 126816.